

Research Article

# Environmentally Benign Green Approach for the Synthesis of IONPs Using *Vicia Faba* Fruit Extract and Their Antioxidant Activities

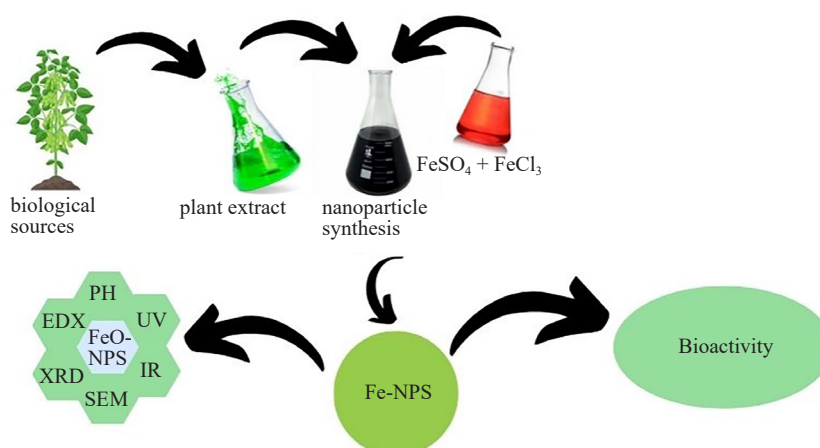
Ruchika Prakash, Ruchi Bharti<sup>\*ID</sup>, Ajay Thakur, Monika Verma, Renu Sharma

Department of Chemistry, University Institute of Sciences, Chandigarh University, Mohali, Punjab, 140413, India  
Email: ruchi.uis@cumail.in

Received: 15 July 2024; Revised: 27 August 2024; Accepted: 29 August 2024

**Abstract:** Iron oxide nanoparticles synthesized from plant materials have garnered considerable attention due to their environmentally friendly nature and wide-ranging applications in various fields. These NPs possess unique attributes, including biocompatibility, low toxicity, catalytic capabilities, and intricate reaction mechanisms, making them highly desirable for diverse biomedical uses. This study presents an innovative green synthesis approach for utilizing the fruit extract of *Vicia faba* (*V. faba*). The synthesized NPs underwent comprehensive characterization using advanced techniques such as Fourier-transform infrared spectroscopy (FTIR), UV-visible spectrophotometry, X-ray diffractometry (XRD), and Scanning Electron Microscope-Energy Dispersive X-ray (SEM-EDX). Notably, the *V. faba* fruit extract served as an effective reducing agent, facilitating the synthesis of Iron oxide nanoparticle (IONP) with well-defined structural and chemical properties. The size of Iron oxide nanoparticles falls between the range of 299.3-527.4 nm. Furthermore, the synthesized Iron oxide nanoparticles were evaluated for their antioxidant activity, revealing promising results against 2,2-diphenyl-1-picrylhydrazyl DPPH and 2,2'-azino-bis (3-ethylbenzothiazoline-6-sulfonic acid) ABTS radicals. These findings highlight the significance of *V. faba* fruit extract in producing IONPs endowed with valuable bioactive properties, offering considerable potential for applications in biomedicine and beyond.

## Graphical Abstract



**Keywords:** green synthesis, iron oxide nanoparticles (IONPs), *vicia faba* fruit extract, bioreducing agents, antioxidant activity, DPPH radicals, nanoparticles (NPs)

## 1. Introduction

In recent years, green synthesis has attracted increasing attention within the nanotechnology domain, driven by the urgent need for sustainable and environmentally friendly approaches to nanoparticles (NPs) production.<sup>1</sup> This paradigm shift in NP synthesis involves utilizing natural sources' reducing and stabilizing properties, such as plant extracts, to fabricate NPs with customized characteristics and minimal environmental impact. Within this context, the present study explores the potential of *Vicia faba* (*V. faba*) fruit extract as a viable reducing and stabilizing agent for the synthesis of Iron oxide NPs (IONPs), offering a pathway toward sustainable nanomaterial synthesis.

IONPs, particularly those in the form of iron oxide, IONPs primarily composed of magnetite ( $\text{Fe}_3\text{O}_4$ ) or maghemite ( $\gamma\text{-Fe}_2\text{O}_3$ ), have attracted significant attention for their superparamagnetic properties and diverse applications in biomedicine, environmental remediation, and materials science.<sup>2</sup> In medicine, they enhance MRI imaging as contrast agents and show promise in targeted drug delivery and hyperthermia cancer therapy, where they generate localized heat to destroy tumor cells. Environmentally, IONPs are effective in water purification and catalysis for pollutant degradation due to their large surface area and adsorption capabilities. Recent research focuses on optimizing their synthesis and functionalization to improve stability, biocompatibility, and application performance in applications. Techniques like co-precipitation, thermal decomposition, and hydrothermal synthesis are used, with surface modifications to enhance dispersion and reduce toxicity. Developing multifunctional IONPs platforms combining diagnostic and therapeutic functions is a promising frontier in nanomedicine.<sup>3</sup> The proposed methodology in this research capitalizes on the rich phytochemicals composition of *V. faba* fruit extract, which possesses bioactive compounds capable of reducing metal ions and stabilizing the resultant NPs. By utilizing plant-derived extracts as green reagents, the synthesis process avoids hazardous chemicals and minimizes energy consumption, aligning perfectly with the principles of green chemistry and sustainable development.<sup>4</sup>

*V. faba*, commonly known as the broad or faba bean, belongs to the Fabaceae family and is known for its distinctive pod-bearing plants. This species is widely cultivated for its edible beans, which have been a staple in various cultures for centuries. Native to North Africa and Southwest Asia, *V. faba* is now grown globally in temperate regions due to its nutritional value and versatility in cooking. The broad bean plant is an annual herbaceous species, typically reaching heights of up to two meters. It features compound leaves with alternately arranged leaflets along the stem. The plant's flowers are notable for their white or purplish hues and are borne in clusters on long stalks. Each flower eventually develops into a pod containing several seeds, which are the edible beans commonly consumed. Beyond its culinary applications, *V. faba* is valued for its agronomic benefits. It is often cultivated as a cover crop or green manure, thanks to its ability to fix nitrogen in the soil, enhancing soil fertility and structure. Additionally, the plant is a valuable forage crop for livestock, providing nutritious fodder. Nutritionally, *V. faba* beans are a rich source of protein, fiber, vitamins, and minerals, making them a healthy addition to various diets. The beans can be eaten fresh, dried, or processed into flour and are used in a wide array of dishes, including soups, stews, salads, and side dishes. From a botanical perspective, *V. faba* exhibits the typical structure of a legume, with nodules on its roots housing nitrogen-fixing bacteria, which contribute to soil nitrogen replenishment. Its cultivation dates back to ancient times, with archaeological evidence of its consumption as early as 6,000 BCE in the Middle East. Overall, *V. faba*, or the broad bean, is significant as a valuable food crop contributor to sustainable agriculture, making it an important plant species with diverse uses and applications.<sup>5</sup> Various phytochemicals, including alkaloids (such as glycosides and convicine), organic acids (like gluconic acid, citric acid, aconitic acid, and azelaic acid), amino acids (e.g., tryptophan), lipids (such as jasmonates), and terpenoids (like dihydrophaseic acid 4'-O- $\beta$ -D-glucopyranoside and another dihydrophaseic acid O-glucopyranoside) are present in *V. faba*. Additionally, phenolic acids (including derivatives of gallic acid, eucomic acid, and their derivatives such as hydroxyeucomic acid, methylhydroxyeucomic acid, and dehydroeucomic acid) and flavonoids (derivatives of O-methylated catechin or epicatechin) have also been identified. These findings align with previous research reported by Valente et al.<sup>6</sup>

One of the notable advantages of employing *V. faba* fruit extract lies in its innate biocompatibility and abundance

in nature, making it a cost-effective and readily available resource for NPs synthesis. Using plant extracts as reducing and stabilizing agents offers a versatile and environmentally benign alternative to conventional chemical methods, mitigating concerns related to toxicity and environmental pollution.<sup>7</sup> Moreover, the simplicity and scalability of the green synthesis approach hold promise for large-scale production of IONPs, further enhancing its applicability in industrial settings. To gain insights into the structural and morphological characteristics of the synthesized IONPs, a comprehensive suite of analytical techniques is employed, including Fourier-transform infrared spectroscopy (FTIR), UV-visible spectrophotometry, X-ray diffractometry (XRD), and Scanning Electron Microscope-Energy Dispersive X-Ray (SEM-EDX) analysis.<sup>8-10</sup> These analyses provide valuable information regarding the composition, crystallinity, and size distribution of the NPs, crucial for understanding their properties and potential applications. Furthermore, the investigation extends to exploring the antioxidant properties of the synthesized IONPs, which play a pivotal role in mitigating oxidative stress-related conditions in biomedical applications.<sup>11-13</sup> The assessment of antioxidant activity offers valuable insights into the potential health benefits of these NPs, underscoring their relevance in pharmaceuticals, nutraceuticals, and functional foods.

This research contributes to advancing the field of green nanotechnology by demonstrating the efficacy of *V. faba* fruit extract in the eco-friendly synthesis of IONPs. By elucidating the structural characteristics and antioxidant properties of the synthesized NPs, the study lays the groundwork for their utilization in diverse fields, including biomedicine, catalysis, and environmental remediation. As the demand for sustainable and biocompatible nanomaterials continues to rise, the findings presented herein hold promise for addressing critical challenges in materials science and promoting a more environmentally conscious approach to NP synthesis.

Despite the progress made in the green synthesis of IONPs, research on using *V. faba* extract for this purpose is limited. The relationship between the extract's bioactive components and the antioxidant activities of the synthesized IONPs has yet to be comprehensively studied. Moreover, optimizing synthesis parameters, such as extract concentration and reaction time, still needs to be explored.

## 2. Materials and methods

### 2.1 Materials

The materials used in this study included ferrous sulfate heptahydrate ( $\text{FeSO}_4 \cdot 7\text{H}_2\text{O}$ ), iron chloride, 2,2-azino-bis-3-ethylbenzothiazoline-6-sulphonic acid (ABTS), 2,2-diphenyl-1-picrylhydrazyl (DPPH), gallic acid, and ascorbic acid, all of which were purchased from Sigma-Aldrich. These chemicals were utilized as reagents and standards in the experimental procedures. In synthesis or solution preparation, de-ionized water is used.

### 2.2 Preparation of extract

The extraction process began with thoroughly washing fresh beans of *V. faba* to eliminate any surface impurities. Following the washing, 100 mg of the fresh beans were finely chopped into small pieces so that water-soluble components dissolved well in water. These bean pieces were then boiled in 100 ml of distilled water for 90 minutes. After boiling the bean pieces in distilled water for 90 minutes, the resulting mixture was subjected to filtration to separate the liquid extract from any solid residues or particulate matter. The filtration process involved passing the boiled bean solution through a filter paper or mesh sieve to retain the extract while removing any insoluble components. Once filtration was complete, the filtrate containing the desired phytochemicals and bioactive compounds was collected and allowed to cool to ambient temperature (approximately 25 °C) before further use in subsequent experiments.

### 2.3 Synthesis of iron oxide NPs

The synthesis of IONPs involved mixing aqueous solutions of  $\text{FeSO}_4$  and  $\text{FeCl}_3$  with the plant extract obtained from *V. faba* beans. Initially, 100 ml of 0.1 M  $\text{FeSO}_4$  and  $\text{FeCl}_3$  in the ratio of 1:1 were combined in a beaker. Subsequently, a burette was filled with 100 ml of the prepared 0.5 g/ml plant extract, which was then slowly added drop-wise to the  $\text{FeSO}_4$  and  $\text{FeCl}_3$  solution while continuously stirring using a magnetic stirrer. Following the reaction, the IONPs were separated from the solution through centrifugation. The precipitate was washed multiple times with

methanol and distilled water to remove residual impurities or unreacted chemicals. Finally, the washed NPs were dried at 30 °C in a hot air oven for 24 hours to obtain the final product in a dry form suitable for further characterization and analysis.

## 2.4 Characterization

The characterization of (IONPs) involved a sequential analysis using various instruments to study different aspects of their properties. Firstly, Fourier-transform infrared spectroscopy (FTIR) was conducted using a Perkin Elmer Spectrum FT-IR Spectrometer to identify functional groups and chemical bonds present in the synthesized NPs. Next, UV-visible spectrophotometry was performed using a Shimadzu UV-1800 instrument to analyze the optical properties and absorbance spectra of the NPs. Subsequently, Scanning Electron Microscopy (SEM) imaging was carried out using a JSM IT 500 instrument to examine the morphology, hydrodynamic diameter, and surface characteristics of the IONPs. Dynamic light scattering (DLS) analysis, utilizing a Mastersizer 3,000 instrument was employed to determine the hydrodynamic diameter distribution and hydrodynamic diameter of the NPs in solution. Lastly, X-ray diffraction (XRD) analysis was performed using a Bruker D8 Advance instrument to investigate the crystallite sizes, phase identification, and crystallinity of the synthesized IONPs.

## 2.5 Antioxidant activity

### 2.5.1 DPPH free radical scavenging assay

The DPPH (2,2-diphenyl-1-picrylhydrazyl) assay measures antioxidant activity based on hydrogen transfer. It utilizes a synthetic, stable radical commonly employed in antioxidant tests. The basic protocol for the DPPH assay involved preparing a DPPH solution by dissolving 4 mg of DPPH in 100 ml of methanol. Subsequently, 3 ml of the DPPH solution was mixed with 200  $\mu$ l of the sample suspension (1mg of IONPs were dissolved in 1mL of methanol and then sonicated to get uniform suspension), thoroughly mixed, and incubated in the dark for 30 minutes. The absorbance of the DPPH solution at 517 nm<sup>14-15</sup> and the reduction of the DPPH radicals by an antioxidant cause discoloration of the test solution. The antioxidant activity was determined by calculating the percentage of DPPH scavenged using:

$$\% \text{ DPPH Scavenging} = [(A \text{ control} - A \text{ sample})/A \text{ control}] \times 100.$$

A sample represents the absorbance of the IONPs solution mixed with the DPPH solution; A control represents the absorbance of the control solution (DPPH solution without IONPs).

### 2.5.2 ABTS radical scavenging assay

ABTS (2,2'-azino-bis (3-ethylbenzothiazoline-6-sulfonic acid)) functions as a cationic complex molecule and a radical scavenger. Various assays are available for testing antioxidant activity based on ABTS radical cation. Using a UV-visible spectrophotometer, the absorbance of the ABTS solution was measured at 734 nm<sup>14-16</sup> both before and after adding the NP suspension. The percentage of ABTS scavenging, indicating antioxidant activity, was calculated using the formula:

$$\% \text{ ABTS Scavenging} = (A - B)/A \times 100,$$

A = absorbance of ABTS,

B = absorbance of ABTS and sample solution.

### 2.5.3 Total antioxidant activity evaluation test

The total antioxidant capacity (TAC) assay focuses on evaluating the compound's ability to reduce  $\text{Mo}^{6+}$  to  $\text{Mo}^{5+}$ , particularly in acidic conditions, measured spectrophotometrically at 695 nm.<sup>17</sup> This reduction process serves as an indicator of the antioxidant potential of the tested compounds. This assay's significant characteristic is the sample solution's observable color change, transitioning from its initial state to a distinct pale green hue. In our study, in this reduction process, the synthesized nanoparticles demonstrated relatively low efficacy, i.e.,  $9 \pm .02\%$ , compared to Gallic

acid, i.e., 82.05%.

### 3. Results and discussion

The gradual addition of the plant extract to the metal ion solution allowed for a controlled reaction between the phytochemicals present in the extract and the metal ions, facilitating the formation of IONPs. The observed color change and precipitation of NPs served as visual indicators of the reaction progress. The formation of IONPs was confirmed through subsequent characterization techniques.

#### 3.1 Characterization of IONPs by UV-Vis spectroscopy and FTIR

The UV-Vis spectrum of the synthesized IONP was recorded at room temperature and analyzed to elucidate the optical properties of the NPs. The spectrum, depicted in Figure 1, exhibited an absorption peak at approximately 277 nm. This prominent absorption peak indicates the presence of IONPs. This observation aligns closely with the absorption peak at 298-301 nm shown in previous research reported by P. Karpagavinayagam and C. Vedhi.<sup>18</sup> The observed absorption in the UV-Vis spectrum can be attributed to the surface plasmon resonance (SPR) phenomenon, which occurs when the collective oscillation of free electrons in the NPs interacts with incident electromagnetic radiation in the ultraviolet-visible range. The specific wavelength of the absorption peak provides valuable information about the size, shape, and optical properties of the NPs. In this case, the absorption peak at 277 nm suggests the formation of IONPs with a characteristic absorption profile in the UV-Vis region. Further analysis and characterization techniques can provide additional insights into the size distribution and morphology of the synthesized IONPs, complementing the information obtained from the UV-Vis spectrum.

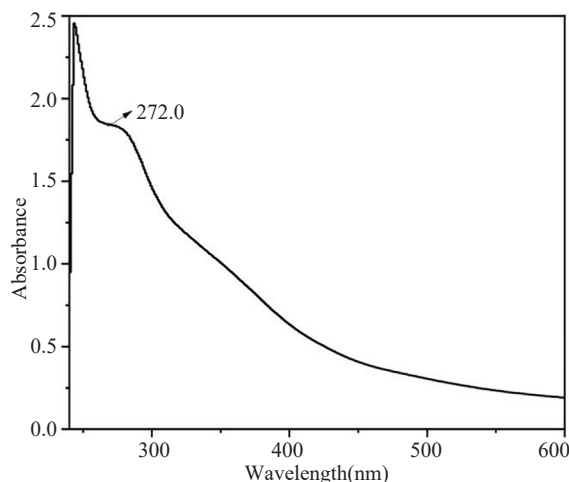


**Figure 1.** UV-Vis spectra for iron oxide NPs

In the Fourier-transform infrared spectroscopy (FTIR) analysis of the synthesized IONPs, distinct peaks were observed at specific wave numbers (Figure 2). The peaks at  $657\text{ cm}^{-1}$  and  $419\text{ cm}^{-1}$  ensure the presence of iron oxide in the sample. This observation aligns closely with previous research findings reported by Samson et al.<sup>19</sup> The broad absorbance at  $3,228\text{ cm}^{-1}$  is characteristic of the O-H group in alcohols and phenolic compounds.<sup>20</sup> Additionally, peaks at  $1,606\text{ cm}^{-1}$  and  $1,058\text{ cm}^{-1}$  suggest C = C stretching vibrations and C-O stretching vibrations at  $2,122\text{ cm}^{-1}$  due to the variable stretching of alkyne groups, respectively. These peaks are consistent with organic functional groups, such as alkenes and alcohols, which may be associated with the stabilizing agents or capping agents used during the synthesis process,<sup>21,22</sup> providing evidence of the formation of IONPs. These FTIR spectra provide valuable insights into the chemical composition and bonding characteristics of the synthesized IONPs, further confirming their successful synthesis.

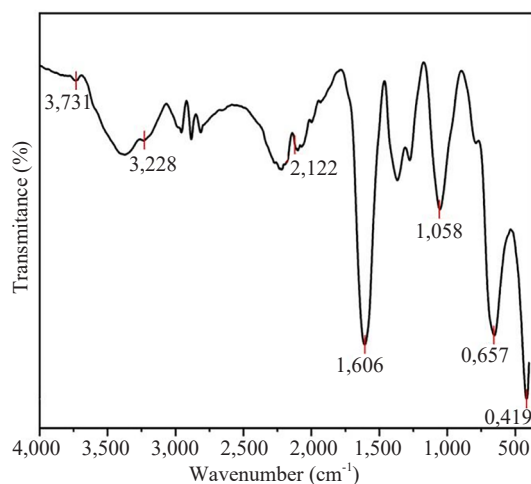


**Figure 2.** For FTIR spectra for iron oxide NPs

### 3.2 Scanning electron microscope-energy dispersive X-Ray (SEM-EDX)

The morphology of the synthesized IONPs was meticulously examined using scanning electron microscopy (SEM) to elucidate their structural characteristics. SEM imaging, depicted in Figure 3, unveiled the intricate irregularities and surface features of the NPs, showcasing their diverse sizes and shapes. Energy-dispersive X-ray spectroscopy (EDS) analysis was meticulously conducted to ascertain the elemental composition of the NPs. As shown in Figure 4, the EDS spectrum exhibited prominent peaks corresponding to the elemental constituents, namely iron (Fe) and oxygen (O), validating their presence within the sample. Moreover, quantitative assessment of the EDS data revealed atomic percentages, with oxygen accounting for 34.98% and iron comprising 65.02% of the elemental composition. These findings corroborated the synthesis of IONPs and provided valuable insights into their elemental composition.

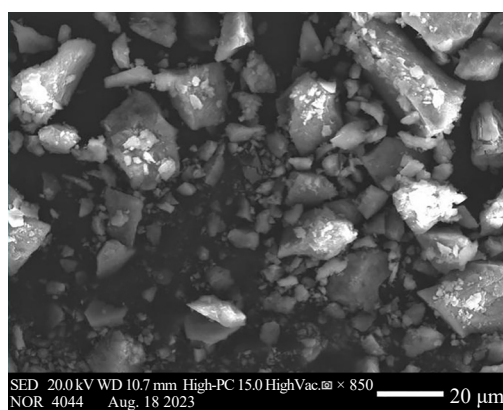


**Figure 3.** SEM images of synthesized IONPs

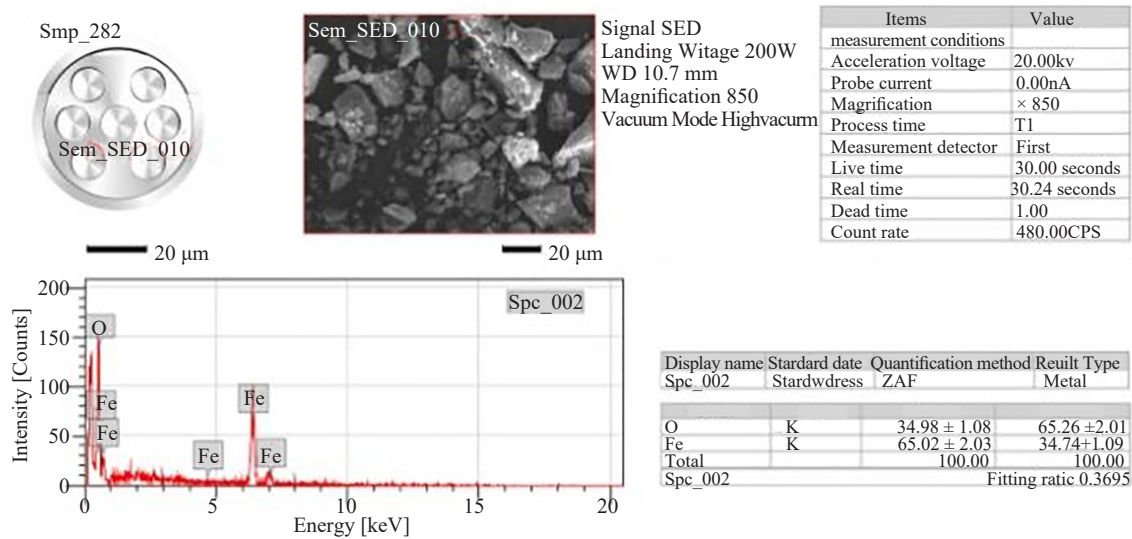


Figure 4. EDX analysis of synthesized IONPs

### 3.3 Dynamic light scattering (DLS)

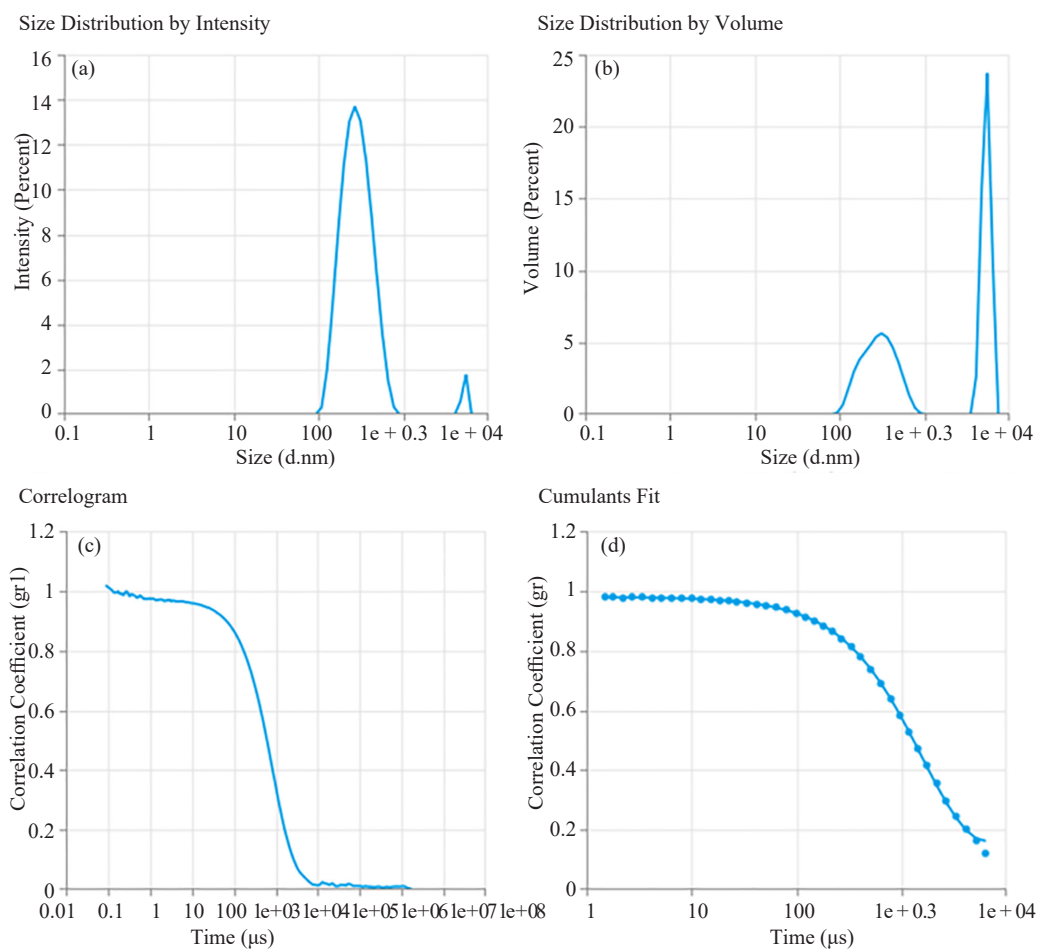


Figure 5. Size Distribution (a), (b), Correlogram (c), and Cumulants fit diagram (d)

The results obtained from the NPs size distribution analysis (shown in Figure 5) provide valuable insights into the sample's characteristics. The Z-average, or the intensity-weighted average hydrodynamic diameter, is calculated to be 297.1 nm. Considering their respective intensities, this value represents the mean size of the NPs in the sample. A Z-average of 297.1 nm suggests that most NPs in the sample fall within this size range.

The polydispersity index (PI) measures a sample's distribution width of hydrodynamic diameters. A PI value of 0.2788 indicates a relatively narrow size distribution, implying that most NPs in the sample have similar sizes. A lower PI value suggests a more uniform distribution of hydrodynamic diameters, which is desirable in many applications as it ensures consistent performance. The intercept value of 0.9794 reflects the linearity of the size distribution curve obtained from the analysis. A value of 1 indicates a linear relationship between hydrodynamic diameter and intensity, indicating a well-defined distribution pattern. The fit error, with a value of 0.001299, indicates the accuracy of the size measurement. A low fit error suggests that the size distribution curve obtained from the analysis closely matches the actual distribution of NPs in the sample, enhancing the reliability of the results. The "In Range (%)" parameter indicates that 92.7% of NPs are within the desired size range, indicating high uniformity in the sample. Finally, the analysis identifies two distinct peaks in the size distribution curve. Peak 1, centered at 299.3 nm, represents a cluster of NPs with a specific size range, while Peak 2, centered at 527.4 nm, indicates another cluster of NPs with a different size range. Understanding the composition and properties of NPs within these size ranges is crucial for determining their potential applications and optimizing their performance in various fields.

### 3.4 X-ray diffraction (XRD)

The X-ray diffraction (XRD) analysis of the synthesized IONPs provides crucial insights into their structural properties, revealing a predominantly amorphous nature. The diffraction pattern is characterized by a broad, diffuse hump rather than sharp, well-defined peaks (Figure 6), which is a clear indication of the lack of long-range atomic order typically associated with crystalline materials. The absence of distinct peaks suggests that the NPs do not possess a significant degree of crystallinity, implying that the atoms within the NPs are arranged in a disordered manner.

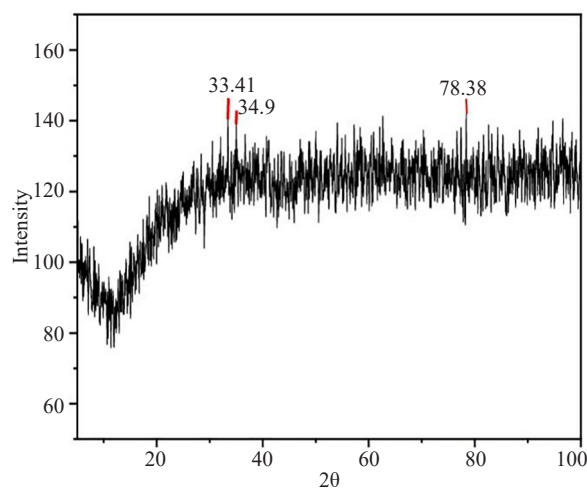


Figure 6. XRD pattern of the IONPs

This amorphous structure contrasts with what would be expected in fully crystalline iron oxide phases such as magnetite ( $\text{Fe}_3\text{O}_4$ ) or maghemite ( $\gamma\text{-Fe}_2\text{O}_3$ ), where sharp and intense peaks corresponding to specific crystal planes would be present. However, the XRD pattern does show slight indications of peaks around  $33.41^\circ$ ,  $34.9^\circ$ , and  $78.38^\circ$ , which may suggest the presence of small, poorly ordered crystalline domains or regions of low crystallinity within the amorphous matrix. This low crystallinity is insufficient to dominate the overall structure, which remains amorphous.

### 3.5 Antioxidant

The analysis of the antioxidant activity of IONPs exhibited significant scavenging activity against ABTS radicals, with a value of  $(91 \pm 0.02)\%$ , indicating their potent antioxidant capability. However, their total antioxidant capacity (TAC) was relatively lower at  $(9 \pm 0.02)\%$  compared to standard antioxidants such as ascorbic acid and Gallic acid. Ascorbic acid demonstrated slightly higher ABTS scavenging activity at  $(95.63 \pm 0.15)\%$ , while Gallic acid exhibited a comparable level at  $(94.93 \pm 0.25)\%$ . Interestingly, IONPs demonstrated comparable DPPH scavenging activity ( $90 \pm 0.02\%$ ) to ascorbic acid ( $92.92 \pm 0.16\%$ ) and Gallic acid ( $93.68 \pm 0.41\%$ ). These findings highlight the potential of IONPs as effective antioxidants, particularly in scavenging ABTS and DPPH radicals. This suggests their suitability for various biomedical applications. Additionally, a comparison of antioxidant activity with literature data is presented in Table 1, further emphasizing the efficacy of IONPs in these roles.

**Table 1.** Comparison of antioxidant activity of IONPs with literature

sample	ABTS	DPPH	TAC	Reference
IONPs synthesized by <i>V. faba</i>	$(91 \pm 0.02)\%$	$(9 \pm 0.02)\%$	$(90 \pm 0.02)\%$	Present research
IONPs synthesized by <i>Bacillus circulans</i>	39.44%	35.44%	-	23
IONPs synthesized by <i>Coriandrumsativum L.</i>	-	32.54% to 84.28%	-	24
IONPs synthesized by the aqueous extract of <i>Penicillium spp.</i>	-	63%	-	25
IONPs synthesized by <i>Inedible borassusflabellifer</i>	-	43.04% to 85.53%	-	26

## 4. Conclusion

In conclusion, this research successfully demonstrates an environmentally benign green synthesis approach for IONPs using *V. faba* fruit extract. The synthesized NPs exhibited promising antioxidant activity, with significant scavenging effects against ABTS and DPPH radicals, showcasing their potential for biomedical applications. The use of *V. faba* extract as a reducing and stabilizing agent underscores the feasibility of sustainable NP production. It highlights the extract's rich phytochemicals profile as instrumental in achieving well-defined IONPs with favorable bioactive properties. Future work will focus on exploring the biomedical applications of these NPs, particularly in drug delivery systems and cancer therapy, where their biocompatibility and antioxidant properties can be further harnessed. Additionally, expanding this green synthesis method to produce other metal oxide NPs will be explored to broaden its applicability in diverse fields such as catalysis, environmental remediation, and sensor development.

## Acknowledgment

The authors are thankful to the Department of Chemistry, Chandigarh University, for providing the basic research facility for this research.

## Conflict of interest

The authors declare there is no conflict of interest at any point with reference to research findings.

## References

- [1] Thakur, A.; Verma, M.; Bharti, R.; Sharma, R. Recent advancement in the green synthesis of silver NPs. *Curr. Chin. Sci.* **2023**, *3*(5), 322-348.
- [2] Ajinkya, N.; Yu, X.; Kaithal, P.; Luo, H.; Somani, P.; Ramakrishna, S. Magnetic iron oxide nanoparticle (IONP) synthesis to applications: Present and future. *Mater.* **2020**, *13*(20), 4644.
- [3] Akintelu, S. A.; Oyebamiji, A. K.; Olugbeko, S. C.; Folorunso, A. S. Green synthesis of iron oxide NPs for biomedical application and environmental remediation: A review. *Eclectic Chemistry* **2021**, *46*(4), 17-37.
- [4] Dahl, J. A.; Maddux, B. L.; Hutchison, J. E. Toward greener nanosynthesis. *Chem. Rev.* **2007**, *107*(6), 2228-2269.
- [5] López-Bellido, F. J.; López-Bellido, L.; López-Bellido, R. J. Competition, growth and yield of faba bean (*Vicia faba* L.). *Eur. J. Agron.* **2005**, *23*(4), 359-378.
- [6] Valente, I. M.; Cabrita, A. R.; Malushi, N.; Oliveira, H. M.; Papa, L.; Rodrigues, J. A.; Maia, M. R. Unravelling the phytonutrients and antioxidant properties of European *Vicia faba* L. seeds. *Int. Food Res.* **2019**, *116*, 888-896.
- [7] Khan, T.; Ullah, N.; Khan, M.A.; Nadhman, A. Plant-based gold NPs; a comprehensive review of the decade-long research on synthesis, mechanistic aspects, and diverse applications. *Adv. Colloid Interface Sci.* **2019**, *272*, 102017.
- [8] Venkatalakshmi, N.; Kini, H. J.; Naik, H. S. B. Green-synthesized nickel oxide nanoparticles: Magnetic and biomedical applications. *Inorg. Chem. Commun.* **2023**, *151*, 110490.
- [9] Singh, K.; Nancy, B. M.; Singh, G.; Mubarak, N. M.; Singh, J. Light-absorption-driven photocatalysis and antimicrobial potential of PVP-capped zinc oxide NPs. *Sci. Rep.* **2023**, *13*(1), 13886
- [10] Golthi, V.; Kommu, J. An eco-friendly and sustainable method for producing Fe<sub>3</sub>O<sub>4</sub> NPs using jatropha podagrica leaf extract for efficient dye degradation and antibacterial uses. *Hybrid Advances* **2023**, *4*, 100110
- [11] Mohamed, N.; Hessen, O. E.; Mohammed, H. S. Thermal stability, paramagnetic properties, morphology and antioxidant activity of iron oxide NPs synthesized by chemical and green methods. *Inorg. Chem. Commun.* **2021**, *128*, 108572
- [12] Vitta, Y.; Figueroa, M.; Calderon, M.; Ciangherotti, C. Synthesis of Iron oxide NPs from aqueous extract of eucalyptus robusta and evaluation of antioxidant and antimicrobial activity. *Mater. Sci. Energy Technol.* **2020**, *3*, 97-103.
- [13] Mirza, A. U.; Kareem, A.; Nami, S. A.; Khan, M. S.; Rehman, S.; Bhat, S. A.; Nishat, N. Biogenic synthesis of Iron oxide NPs using *agrewiaoptiva* and *prunuspersicaphyto* species: Characterization, antibacterial and antioxidant activity. *J. Photochem. Photobiol. B.* **2018**, *185*, 262-274.
- [14] Thakur, A.; Bharti, R.; Verma, M.; Sharma, R. Sharma, A.; Gupta, A.; Sharma, V. Ultra-sonicated one-pot synthesis of potent bioactive biscoumarin and polycyclic pyranodichromenone scaffolds in aqueous media: A complementary tool to organic synthesis. *Synthesis* **2023**, *55*(19), 3129-3144.
- [15] Thakur, A.; Verma, M.; Setia, P.; Bharti, R.; Sharma, R.; Sharma, A.; Bansal, R. DFT analysis and in vitro studies of isoxazole derivatives as potent antioxidant and antibacterial agents synthesized via one-pot methodology. *Res. Chem. Intermed.* **2023**, *49*(3), 859-883.
- [16] Verma, M.; Thakur, A.; Kapil, S.; Sharma, R.; Sharma, A.; Bharti, R. Antibacterial and antioxidant assay of novel heteroaryl-substituted methane derivatives synthesized via ceric ammonium nitrate (CAN) catalyzed one-pot green approach. *Mol. Divers.* **2023**, *27*(2), 889-900.
- [17] Basavegowda, N.; Idhayadhulla, A.; Lee, Y. R. Phyto-synthesis of gold nanoparticles using fruit extract of *hoveniadulcis* and their biological activities. *Ind Crop Prod.* **2014**, *52*, 745-751.
- [18] Karpagavinayagam, P.; Vedhi, C. Green synthesis of ironoxide NPs using *avicennia marina* flower extract. *Vacuum.* **2019**, *160*, 286-292.
- [19] Aisida, S. O.; Madubuonu, N.; Alnasir, M. H.; Ahmad, I.; Botha, S.; Maaza, M.; Ezema, F. I. Biogenic synthesis of iron oxide nanorods using *moringaoleifera* leaf extract for antibacterial applications. *Appl. Nanosci.* **2020**, *10*, 305-315.
- [20] Song, J. Y.; Jang, H. K.; Kim, B. S. Biological synthesis of gold nanoparticles using *magnolia kobus* and *diopyros kaki* leaf extracts. *Process Biochem.* **2009**, *44*(10), 1133-1138.
- [21] Bhuiyan, M. S. H.; Miah, M. Y.; Paul, S. C.; Aka, T. D.; Saha, O.; Rahaman, M. M.; shaduzzaman, M. A. Green synthesis of IONPs using *carica papaya* leaf extract: Application for photocatalytic degradation of remazol yellow RR dye and antibacterial activity. *Heliyon.* **2020**, *6*(8), e04603.
- [22] Sathya, K.; Saravanathamizhan, R.; Baskar, G. Ultrasound assisted photosynthesis of iron oxide nanoparticle. *Ultrason. Sonochem.* **2017**, *39*, 446-451.
- [23] Rabani, G.; Dilshad, M.; Sohail, A.; Salman, A.; Ibrahim, S.; Zafar, I.; Arshad, H. M. Extracellular synthesis of

- iron oxide nanoparticles using an extract of bacillus circulans: Characterization and in vitro antioxidant activity. *J. Chem.* **2023**, 2023(1), 4659034.
- [24] Singh, K.; Chopra, D. S.; Singh, D.; Singh, N.; Optimization and ecofriendly synthesis of iron oxide nanoparticles as a potential antioxidant. *Arab. J. Chem.* **2020**, 13(12), 9034-9046.
- [25] Zakariya, N. A.; Majeed, S.; Jusof, W. H. W. Investigation of antioxidant and antibacterial activity of iron oxide nanoparticles (IONPS) synthesized from the aqueous extract of penicillium spp. *Sens. Int.* **2022**, 3, 100164.
- [26] Sandhya, J.; Kalaiselvam, S. Biogenic synthesis of magnetic iron oxide nanoparticles using inedible borassusflabellifer seed coat: Characterization, antimicrobial, antioxidant activity and in vitro cytotoxicity analysis. *Mater. Res. Express.* **2020**, 7(1), 015045.